Heat Transfer Engineering

ISSN: (Print) (Online) Journal homepage: https://www.tandfonline.com/loi/uhte20

Numerical Investigation on Flow Pattern, Heat Transfer and Pressure Drop Characteristics of Flow Boiling with Discrete Heat Sources

Ping Yang, Weihao Ling, Ke Tian, Min Zeng & Qiuwang Wang

To cite this article: Ping Yang, Weihao Ling, Ke Tian, Min Zeng & Qiuwang Wang (2023): Numerical Investigation on Flow Pattern, Heat Transfer and Pressure Drop Characteristics of Flow Boiling with Discrete Heat Sources, Heat Transfer Engineering, DOI: 10.1080/01457632.2023.2213997

To link to this article: https://doi.org/10.1080/01457632.2023.2213997

HEAT TRANSFER ENGINEERING
https://doi.org/10.1080/01457632.2023.2213997

Taylor & Francis
Taylor & Francis Group

Numerical Investigation on Flow Pattern, Heat Transfer and Pressure Drop Characteristics of Flow Boiling with Discrete Heat Sources

Ping Yang, Weihao Ling, Ke Tian, Min Zeng, and Qiuwang Wang

Key Laboratory of Thermo-Fluid Science and Engineering, Ministry of Education, Xi'an Jiaotong University, Xi'an, Shaanxi, China

ABSTRACT

Heat dissipation and temperature uniformity are one of the key technologies for electronic equipment. With the rapid growth of computing demand and the wide application of multi-chip devices, heat sources are distributed discretely in space. Therefore, the flow boiling in the mini-channel with two discrete heat sources is investigated in this study. The effects of heat source distribution, inlet fluid temperature and channel diameter on flow pattern, heat transfer and pressure drop are discussed in detail. The results show that intermittent flow tends to form around discrete heat sources, especially near the heat source which is far from the channel inlet. Moreover, the distance between discrete heat sources shouldn't be too close to avoid heat concentration, nor too far to make full use of latent heat. When the distance between two heat sources is 70 mm, the temperature distribution is appropriate, and the heat dissipation is the best in this study. For the discrete heat source far from the inlet, the heat transfer coefficient increases significantly when the inlet fluid temperature increases due to the preheating of another heat source.

Introduction

With the mature development of integrated circuit technology, the heat flux of electronic products is increasing sharply. Karayiannis and Mahmoud [1] predicted that the average heat flux of computer chips would reach 2-4.5 MW/m^2 in 2026. Undoubtedly, if the heat can't be dissipated efficiently, the high heat flux will make the chip temperature increase, which is pernicious to the electronic equipment lifetime. Therefore, more effective thermal management is urgently required.

Compared with single-phase flow, flow boiling has great heat transfer efficiency and can make the surface temperature more uniform due to the latent heat. Therefore, a great quantity of studies on heat transfer of flow boiling have been carried out in electronic industries and other applications. Sumith et al. [2] found that existing flow boiling correlations underpredicted the heat transfer at a heat flux less than 200 kW/m^2, so they came up with a new method to predict the heat transfer coefficient of water boiling based on their experimental data. Similarly, Lillo et al. [3] investigated the flow boiling of propane through experiments. They proposed a modified method to predict heat transfer and assessed available prediction tools of dry out vapor qualities and pressure drop. Niu et al. [4] focused on the flow boiling heat transfer performance of R134a in the helically coiled tube. They found that nucleate boiling played a significant role but convective boiling would be weakened at high vapor quality, and they proposed a new correlation of heat transfer coefficient for the above conditions (heat flux $q = 2\text{-}60\ kW/m^2$; mass flux $G = 182.9\text{-}800\ kg/(m^2{\cdot}s)$; pressure $p = 0.41\text{-}1.1$ MPa). Besides the effect of thermal properties, the channel structure is also a significant factor affecting flow boiling. Soupremanien et al. [5] conducted experiments to discuss the influence of aspect ratio on horizontal flow boiling with the same hydraulic diameter (1.4 mm). They pointed out that the channel with a smaller aspect ratio had a higher heat transfer coefficient if the heat flux was low, but the result was contrary for high heat flux conditions. However, Özdemir et al. [6] confirmed that the channel with the smaller aspect ratio showed greater heat dissipation when the heat flux was up to 480-500 kW/m^2. Yen et al. [7] and Deng et al. [8] studied the heat transfer characteristic of flow boiling in the channel with different cross sections. They indicated that square

CONTACT Min Zeng zengmin@mail.xjtu.edu.cn Key Laboratory of Thermo-Fluid Science and Engineering, Ministry of Education, Xi'an Jiaotong University, Xi'an, Shaanxi, 710049, China

Nomenclature

a	distance between the heat source 1 center point and section A-A, m
b	distance between the heat source 2 center point and section A-A, m
c_p	specific heat capacity, J/(kg·K)
d	channel diameter, m
E	specific energy, J/kg
F	volume force induced by interface interaction, N/m^3
g	gravitational acceleration, m/s^2
G	mass flux, kg/(m^2·s)
h	latent heat, J/kg
k	thermal conductivity, W/(m·K)
p	pressure, Pa
q	heat flux, W/m^2
r	axial coordinates along the radial direction, m
S_e	energy source term, J/(m^3·s)
S_l	mass transfer rate between the liquid and vapor phase, kg/(m^3·s)
S_v	mass transfer rate between the liquid and vapor phase, kg/(m^3·s)
t	time, s
T	temperature, K
v	velocity, m/s
VOF	volume of fluid
x	Vapor quality, 1
z	Axial coordinate along the flow direction, m

Greek Symbols

α	phase fraction, 1
β	vapor volume fraction, 1
θ	axial coordinate along the circumferential direction, rad
κ	interface curvature, m^{-1}
λ	relaxation factor, s^{-1}
μ	viscosity, Pa·s
ρ	density, kg/m^3
σ	surface tension coefficient, N/m

Subscripts

eff	effective
l	liquid phase
v	vapor phase
sat	saturation

cross section and unique Ω-shaped cross section were beneficial to enhance the heat transfer of flow boiling. However, most experimental studies difficultly investigate the details of flow pattern in the mini and micro-channel limited by experimental measurement technologies.

Due to the development of computer technology, numerical simulation can overcome the shortcomings of experimental studies and reveal some local characteristics. Kunkelmann and Stephan [9] successfully simulated the vapor bubble growth and detachment from the heated surface based on the volume of fluid model (VOF) and validated the contact line model in boiling heat transfer. La Forgia et al. [10] revealed the evolution of vapor bubble growth in flow boiling using the diffuse interface method. The results showed that the bubbles grew almost linearly during evaporation, and the surface tension could keep bubbles spherical. Huang et al. [11] numerically analyzed the heat transfer, pressure drop and flow pattern of flow boiling in the mini-channel for different conditions. They summarized that the heat transfer coefficient would increase with the increase of vapor volume fraction while the vapor volume fraction ranged between 0.2 and 0.5. Similarly, Yin et al. [12] numerically investigated the heat transfer in a mesoscale separated heat pipe. They divided the flow pattern into four types in the mesoscale vertical tube and found that nucleate boiling is the main boiling form at low heat flux. Lee et al. [13] investigated flow boiling in the finned microchannel by numerical method and optimized the radiator design to enhance the flow boiling heat transfer. The results indicated that when the fin height was 0.03 mm, the shorter the fin length, the better heat transfer. Luo et al. [14] numerically studied the hydrodynamics and heat transfer performance of annular flow boiling in a narrow rectangular microchannel. They pointed out that increasing inlet vapor quality and wall heat flux were able to enhance heat transfer because the liquid film thickness was decreased. Shao et al. [15] performed a fundamental numerical investigation on the flow boiling of R410A and clarified the effects of mass flux and heat flux on heat transfer. They found that heat transfer coefficient increased with the mass flux increasing but was slightly influenced by heat flux. However, the above studies rarely consider the effect of non-uniform heating on flow boiling.

Moreover, to improve performance, multichip devices have been widely used, which makes heat source distribute discretely in space. Jeindel et al. [16] performed a forced convection boiling experiment for an in-line 1×10 array of discrete heat sources without deep flow pattern investigation. They found that the maximum temperature difference between heat sources was insensitive to channel height under fully developed nucleate boiling conditions. Cho et al. [17, 18] investigated cooling performance and pressure drop in the micro-channel heated by 9 discrete heat sources. The results indicated that the channel with the trapezoidal header was the best design considering temperature distribution and pressure drop, but they

didn't show the effect of non-uniform on flow pattern either. Ritchey et al. [19] conducted an experimental investigation to explore the flow boiling in micro-channel with non-uniform heating using individual heaters of 5×5 arrays. The results showed that for the non-uniform heating case, the local flow regimes and heat transfer coefficients deviated significantly from the uniformly heated case. Kurose et al. [20, 21] studied the heat transfer characteristics and the refrigerant flow distribution in the parallel channels heated unequally in the air conditioning system. They developed correlation equations predicting mass flow rates and inlet vapor qualities under unequally heated conditions. However, they focused on the non-uniform heating between two channels, rather than discrete heat source heating. Heat transfer performance and instability in parallel channels with discrete heat sources were studied in our previous work [22], but the effect of discrete heat source distribution on heat transfer was not analyzed essentially and other influences were not discussed. Besides, flow pattern and pressure drop characteristics of flow boiling in the channel with discrete heat sources were not investigated either in our previous work.

It can be seen from the above literature that more comprehensive and profound investigations are needed to understand the two-phase flow characteristics better especially for flow pattern when the channel is heated with discrete heat sources. Consequently, flow pattern, heat transfer and pressure drop characteristics of flow boiling with discrete heat sources are investigated in detail in this study. Besides, the effects of heat source distribution, inlet fluid temperature and channel diameter on the above characteristics have been analyzed. This study is expected to provide a further understanding of flow boiling with discrete heat sources and some optimization suggestions for the two-phase flow cooling system.

Numerical model and validation

Physical model

The flow boiling in a mini-channel heated by two discrete heat sources is investigated. In order to save computing resources, the physical model can be reasonably simplified as a two-dimensional axisymmetric model. The computational configurations are shown in Figure 1, where the channel length is 200 mm, and two adiabatic segment lengths are both 90 mm. The solid thickness is 0.3 mm. Section A-A is the channel symmetry plane, and a or b represents the distance between the heat source center point and section A-A. This study assumes that $a = b$ and the heat source length is 20 mm. Besides, the velocity and pressure boundary conditions are applied in the computational domain inlet and outlet. Inlet velocity is considered uniform which is 0.2 m/s. The refrigerant operating pressure is 101325 Pa. Channel is heated by two discrete heat sources with a constant heat flux of 30000 W/m^2. Other walls are cooled by natural convection and the ambient temperature is 293.15 K. The solid is aluminum. The saturation temperature of R141b is 32 °C when the pressure is 101325 Pa, and the chip temperature is usually expected to be less than 80 °C. Therefore, cooling electronic equipment can be realized at low pressure when the fluid is R141b, which can improve the safety of the cooling system. Thus, R141b is studied in this study. The thermal properties of R141b are presented in Table 1 [11].

Mathematical model

Governing equations

The two-phase flow is calculated based on the VOF model, and the governing equations are as follows:

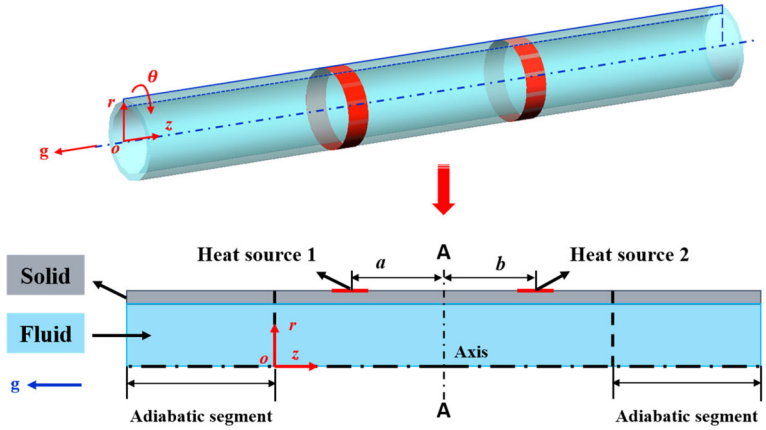

Figure 1. Physical model and computational configuration.

Table 1. Properties of R141b [11].

Property reference	Correlation
Density of liquid	$\rho_l = -0.003\,T^2 - 0.1355\,T + 1538.3$
Density of vapor	$\rho_v = 0.003\,T^2 - 1.6827\,T + 240$
Thermal conductivity of liquid	$k_l = 3e^{-7}T^2 - 0.0005\,T + 0.2033$
Thermal conductivity of vapor	$k_v = 2e^{-7}T^2 - 7e^{-5}T + 0.0096$
Specific heat of liquid	$c_{pl} = -0.008\,T^2 - 3.3\,T + 1458.6$
Specific heat of vapor	$c_{pv} = 0.006\,T^2 - 1.1\,T + 611.8$
Dynamic viscosity of liquid	$\mu_l = 2e^{-8}T^2 - 2e^{-5}T + 0.0035$
Dynamic viscosity of vapor	$\mu_v = 3e^{-11}T^2 + 1e^{-8}T + 3e^{-6}$
Surface tension	$\sigma = 9e^{-8}T^2 - 0.0002\,T + 0.0629$

Mass conservation equation:

$$\frac{\partial \rho}{\partial t} + \nabla \cdot \left(\rho \vec{v}\right) = 0 \tag{1}$$

where ρ and $\vec{v}$ are density and velocity.

Momentum conservation equation:

$$\frac{\partial}{\partial t}\left(\rho \vec{v}\right) + \nabla \cdot \left(\rho \vec{v}\,\vec{v}\right) = -\nabla p + \nabla \cdot \left[\mu_{\text{eff}}\left(\nabla \vec{v} + \left(\nabla \vec{v}\right)^T\right)\right] + \rho \vec{g} + \vec{F} \tag{2}$$

where p, μ_{eff} and $\vec{g}$ are pressure, effective viscosity, and gravitational acceleration respectively. $\vec{F}$ represents the volume force induced by interface interaction. The interface surface tension is calculated by the continuum surface force model proposed by Brackbill et al. [23]. Moreover, the force at the surface can be expressed as a volume force by using the divergence theorem. Thus, $\vec{F}$ is calculated as follows:

$$\vec{F} = \sigma_{\text{lv}} \frac{\alpha_l \rho_l \kappa_v \nabla \alpha_v + \alpha_v \rho_v \kappa_l \nabla \alpha_l}{0.5(\rho_l + \rho_v)} \tag{3}$$

where subscript "1" and "v" represent liquid phase and vapor phase, α is phase fraction and σ_{lv} is surface tension coefficient. If α is 1, the grid is full of liquid phase. If α is 0, the grid is full of vapor phase. If $0<\alpha<1$, there are liquid and vapor phase in the grid. κ_{v} and κ_{l} are interface curvature, which can be written as follows:

$$\kappa_v = -\kappa_l = \nabla \cdot \frac{\nabla \alpha_v}{|\nabla \alpha_v|} \tag{4}$$

Energy conservation equation:

$$\frac{\partial}{\partial t}(\rho E) + \nabla \cdot \left[\vec{v}(\rho E + p)\right] = \nabla \cdot (k_{\text{eff}} \nabla T) + S_e \tag{5}$$

where k_{eff} is effective thermal conductivity and S_{e} is energy source term, which is calculated in the phase change model.

VOF equations:

$$\frac{\partial}{\partial t}(\alpha_v \rho_v) + \nabla \cdot \left(\alpha_v \rho_v \vec{v}\right) = S_v \tag{6}$$

$$\alpha_l + \alpha_v = 1 \tag{7}$$

where S_{v} is the mass transfer rate between the liquid phase and vapor phase due to phase change, which can also be obtained in the phase change model.

According to the VOF model theory, the above fluid thermal properties are defined as follows:

$$\rho = \rho_l \alpha_l + \rho_v \alpha_v \tag{8}$$

$$\mu = \mu_l \alpha_l + \mu_v \alpha_v \tag{9}$$

$$k = k_l \alpha_l + k_v \alpha_v \tag{10}$$

$$E = \frac{\alpha_l \rho_l E_l + \alpha_v \rho_v E_v}{\alpha_l \rho_l + \alpha_v \rho_v} \tag{11}$$

Phase change model

It's essential to use an appropriate phase change model in the flow boiling numerical simulation. Among the existing phase change models, the evaporation-condensation phase change model proposed by Lee [24] is the simplest one to be implemented and is suitable for simulating sub-cooled flow boiling.

Based on the gas dynamics theory, the mass and energy transfer between the liquid phase and vapor phase can be calculated with Equations (12) and (13) in the Lee model.

$$\begin{cases} S_v = \lambda_l \alpha_l \rho_l \dfrac{T - T_{\text{sat}}}{T_{\text{sat}}}, \; S_l = -S_v & T > T_{\text{sat}} \\ S_l = \lambda_v \alpha_v \rho_v \dfrac{T - T_{\text{sat}}}{T_{\text{sat}}}, \; S_v = -S_l & T < T_{\text{sat}} \end{cases} \tag{12}$$

$$S_e = h_{\text{lv}} S_v \tag{13}$$

where h_{lv} is latent heat and T_{sat} means refrigerant saturation temperature. It's noteworthy that relaxation factors λ_1 and λ_{v} are empirical coefficients and should be appropriate for different simulations. If λ_1 and λ_{v} are too small, the interface temperature will deviate from the saturation temperature too much, which will make the simulation results inaccurate. However, the relaxation factors also can't be too large because the simulation convergence will not be guaranteed. Usually, λ_1 and λ_{v} are set from 0.1-100 s^{-1} [25]. In this study, $\lambda_1 = \lambda_{\text{v}}$ are from 0.1-200 s^{-1} in order to avoid computational divergence and ensure that the phase interface temperature is close to the saturation temperature.

Simulation method

Based on the finite volume method, the pressure-based segregated solver PISO is chosen to solve the governing equations. PRESTO! method is used to discretize pressure. The momentum and energy equations are discretized using the second order upwind

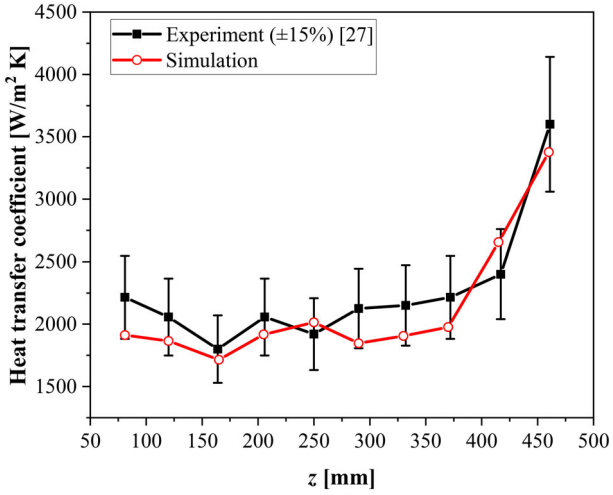

Figure 2. Numerical method validation-heat transfer coefficient comparison between experiment [27] and simulation.

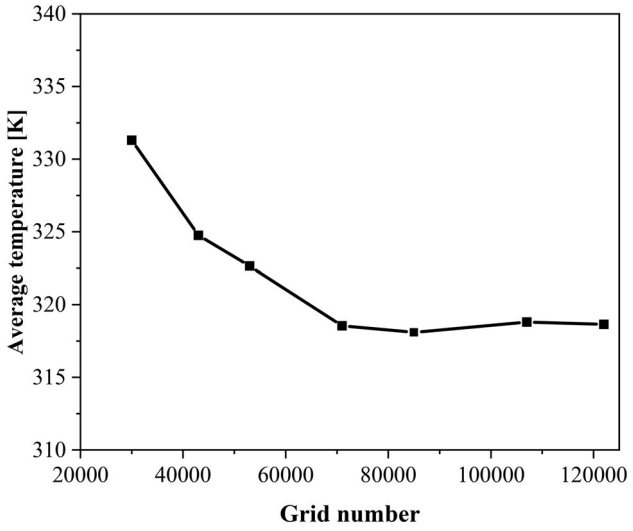

Figure 3. Grid independence test.

scheme. In order to improve simulation accuracy, Green Gauss Node Based method is applied for gradient discretization. Geometric Reconstruction scheme proposed by Youngs [26] is implemented to structure the phase interface. Besides, the SST k - ω turbulence model is employed to calculate turbulence in this study. The calculation is considered as convergent when the residual of energy equation is less than 10^{-6} and other equation residuals are less than 10^{-4}.

Validation of the model

For the sake of simulation accuracy, the simulation results are compared with experimental data, which was obtained by Lin et al. [27] at the heat flux of 30 kW/m^2. Lin et al. investigated the flow boiling of R141b in the vertical mini-channel, where the internal

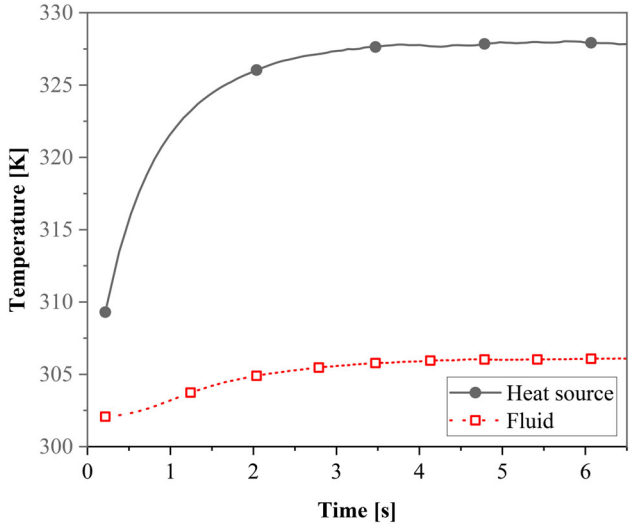

Figure 4. Heat source average temperature and fluid average temperature vary with time.

diameter and length of the channel are 1 mm and 500 mm. Figure 2 shows the comparison of the local heat transfer coefficients along the channel, and the error bars of experimental data are 15% in Figure 2. It can be observed that the numerical results agree well with the experimental data and the maximum relative deviation is less than 15%, so the simulation methods used in this study are correct. In addition, to test grid independence, seven sets of grids are tested as illustrated in Figure 3. The case with 71000 grids is used to consider both the accuracy and convergence rate.

Results and discussion

It's widely known that flow boiling is a complex transient process and ought to be solved with time. However, if the boundary conditions do not change with time, the flow boiling will eventually reach the pseudo steady state, in which the average temperatures of heat sources and fluid fluctuate in a small range, as shown in Figure 4. In industrial applications, the results of flow boiling under the pseudo steady state are paid more attention to, which are significant for heat exchanger design and optimization. So, the heat transfer and pressure drop are discussed under the pseudo steady state in this study.

Flow pattern

Effect of discrete heat sources distribution

When the discrete heat source is used to heat the channel, the heat source distribution is an issue that should be discussed. The inner diameter, heat flux, inlet temperature and velocity are 3 mm, 30000 W/m^2,

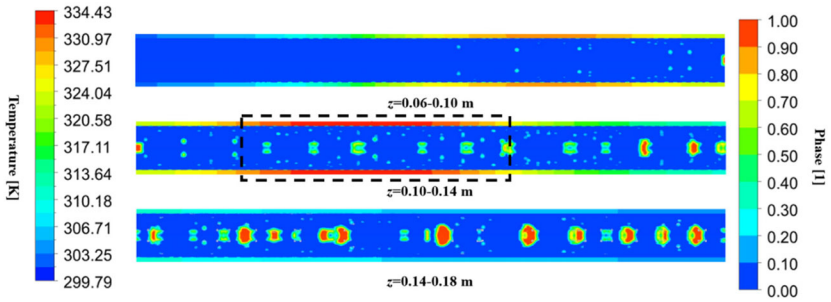

(a) $a = b = 15$ mm

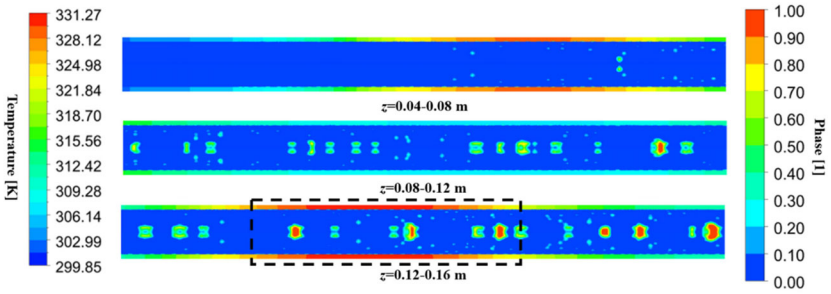

(b) $a = b = 35$ mm

Figure 5. Temperature distribution in solid and phase volume fraction distribution in fluid vary with heat sources distribution when flow time is 6.5 s.

300 K and 0.2 m/s. There are four typical flow patterns in vertical channel which are bubble flow, slug flow, annular flow, and mist flow. In bubble flow, irregularly shaped bubbles are dispersed in the liquid phase. In slug flow, there are typical Taylor bubbles, which look like bullets and have a diameter close to the channel diameter. As for annular flow, the liquid film is attached to the wall, and the vapor phase occupies the channel center. Mist flow means liquid droplets are dispersed in the vapor phase. Figure 5 shows the phase volume fraction distribution in fluid and the temperature distribution in solid when $a = b = 15$ mm and $a = b = 35$ mm at 6.5 s. It should be mentioned that $z = 0$ mm means the channel inlet without the adiabatic segments. Since the refrigerant is subcooled when entering the channel, single-phase flow and subcooled boiling will appear at the beginning. The fluid near the wall is firstly heated to saturation temperature when the fluid gradually approaches the discrete heat source. Then a series of bubbles are generated, which escape from the wall and gather in the center of the channel due to buoyancy, forming a bubble flow. Based on the above boundary conditions, it can be clearly concluded from Figure 5 that the flow pattern is bubbles flow when the flow boiling reaches the pseudo steady state. However, compared Figure 5(a) with Figure 5(b), the behavior of bubbles along the channel is different when the distribution of discrete heat sources changes. When $a = b = 15$ mm, the mature bubbles around discrete heat sources are less than that when $a = b = 35$ mm. In addition, the temperature field in the solid is quite different. The temperature of heat sources decreases obviously when $a = b = 35$ mm compared with that when $a = b = 15$ mm. These phenomena show that compared with continuous heating, the flow pattern and heat transfer are irregular when the channel is heated with discrete heat sources. More detailed information will be discussed in the following sections.

Effect of inlet temperature

In the actual cooling system, the inlet fluid temperature is an important factor affecting flow boiling. Therefore, the effect of inlet fluid temperature on flow pattern is studied in this section.

Simulations are conducted for three inlet temperatures when $a = b = 35$ mm, which are 300 K, 302 K and 303.5 K respectively. Besides, the inner diameter, the heat flux, and the velocity are 3 mm, 30000 W/m^2, and 0.2 m/s. It can be seen from Figure 6 that when the inlet temperature increases to 302 K or 303.5 K, there will be cap flow except for bubble flow. When the inlet temperature is 303.5 K, the cap flow proportion in the whole channel is greater than that when the inlet temperature is 302 K. In addition, the higher the inlet temperature, the closer the cap flow is to the discrete heat sources. This is because the sensible heat

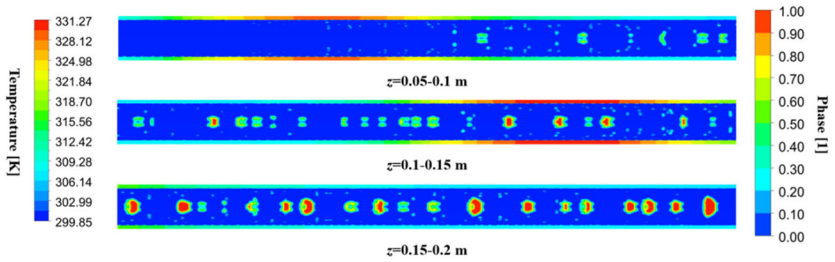

(a) inlet temperature 300 K

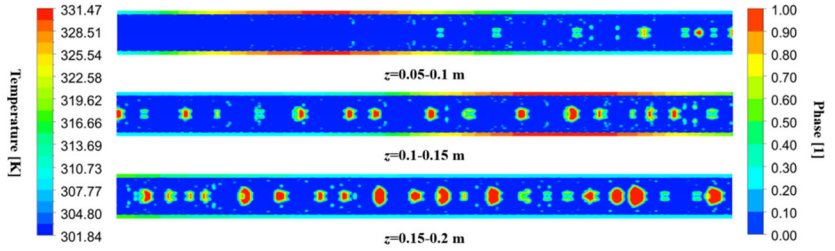

(b) inlet temperature 302 K

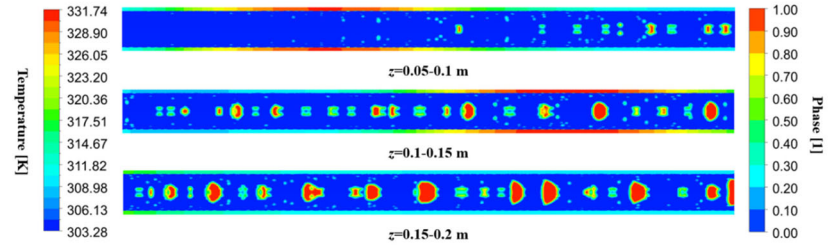

(c) inlet temperature 303.5 K

Figure 6. Temperature distribution in solid and phase volume fraction distribution in fluid vary with inlet fluid temperature when flow time is 6.5 s.

decreases with the increase of fluid inlet temperature, which results in more bubbles. Then, due to the collision and agglomeration of many bubbles, cap flow is gradually formed and accompanied by bubble flow.

Effect of channel diameter

The ratio of the heat transfer surface area to the volume is high in the mini-channel, which is beneficial to improve heat transfer. Therefore, the channel diameter is changed to 2 mm and 1 mm to investigate the effect of channel diameter on flow boiling under discrete heat sources. The heat flux, inlet temperature and velocity are kept at 30000 W/m^2, 300 K and 0.2 m/s when $a = b = 35$ mm.

As shown in Figure 7, different from the flow pattern in the channel with a diameter of 3 mm, some new flow patterns appear in the smaller channel during the development of flow pattern, such as slug flow, intermittent flow and annular flow. When the diameter is 2 mm or 3 mm, more bubbles will gather before escaping from the wall and become larger bubbles. Then, because the influence of surface tension is greater than that of buoyancy, the bubble volume increases significantly in the axial direction rather than radial direction, forming Taylor bubbles. As a result, slug flow is shaped in the fluid between two discrete heat sources or behind the heat source 2. In addition, intermittent flow occurs in the channel, especially near the discrete heat source when the diameter is 1 mm as shown in Figure 7(b), which is detrimental to heat dissipation and circulating flow.

However, as shown in Figure 8, when the flow boiling reaches the pseudo steady state, the flow pattern in the smaller channel will change greatly. The final flow pattern in the channel with a diameter of 3 mm is bubble flow, and the vapor volume fraction is small, but the vapor volume fraction in the channel with a diameter of 2 mm or 1 mm increases sharply to form mist flow. The reason why the flow pattern is so sensitive to the channel diameter is that the density of

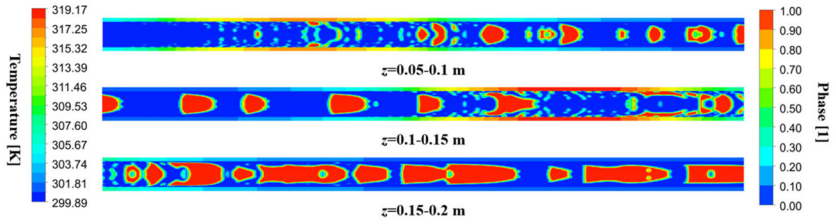

(a) $d = 2$ mm

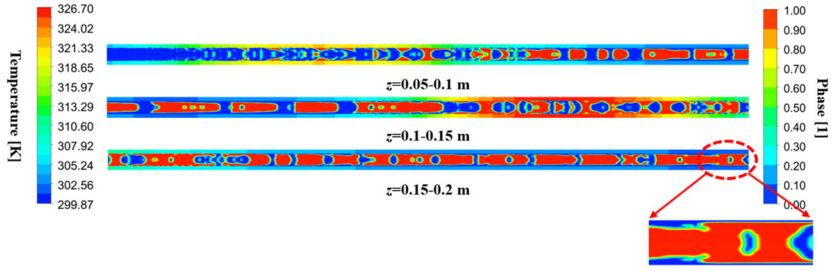

(b) $d = 1$ mm

Figure 7. Temperature distribution in solid and phase volume fraction distribution in fluid vary with channel diameter when flow time is 1 s.

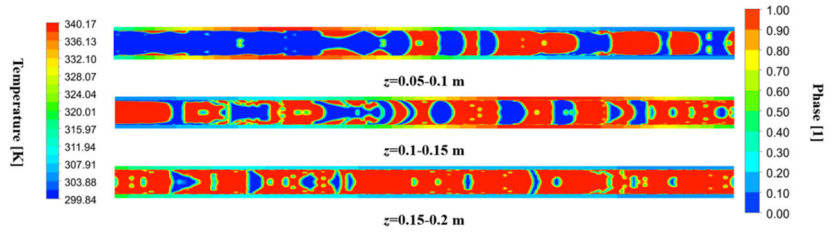

(a) $d = 2$ mm, flow time $t = 6.1$ s

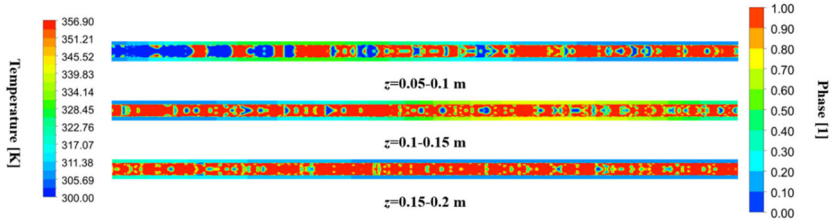

(b) $d = 1$ mm, flow time $t = 2.92$ s

Figure 8. Temperature distribution in solid and phase volume fraction distribution in fluid vary with channel diameter when flow boiling reach pseudo steady state.

R141b varies greatly between the liquid phase and vapor phase. Based on the knowledge of two-phase flow, the relationship between vapor quality and vapor volume fraction is as follows:

$$x = \frac{\beta\rho_g}{\beta\rho_g + (1-\beta)\rho_l} \tag{14}$$

where x is vapor quality and β is vapor volume fraction. Using Equation (14), it can be seen from Figure 9 that a slight change in vapor quality will lead to a drastic change in vapor volume fraction before the vapor quality reaches a small value.

Heat transfer characteristics

Effect of discrete heat sources distribution

It has been mentioned that the temperature of heat sources decreases obviously when the heat source distribution is changed. Hence, to quantitatively illustrate

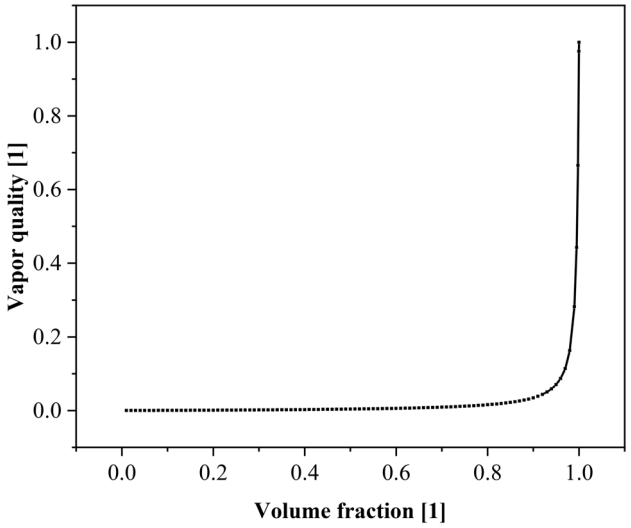

Figure 9. Vapor quality x variation with vapor volume fraction β.

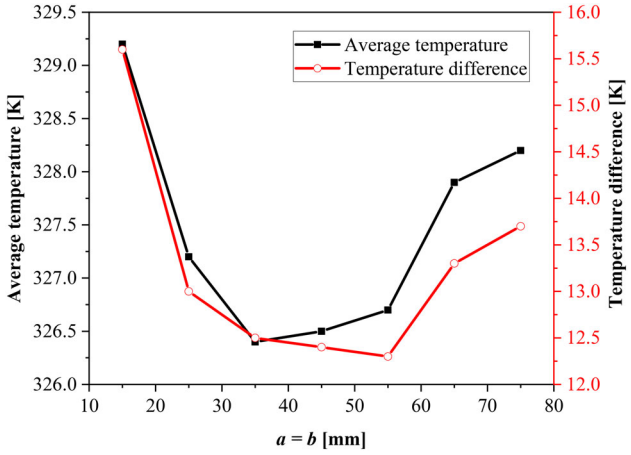

Figure 10. The average temperature of heat sources and temperature difference between heat sources vary with heat sources distribution when flow time is 6.5 s.

the effect of heat source distribution on heat dissipation, Figure 10 shows the average temperature of the heat sources and the temperature difference between the two heat sources. When $a = b = 15/25/65/75$ mm, the average temperature of heat sources far outweighs that when $a = b = 35/45/55$ mm. When $a = b = 35$ mm, the average temperature of heat source is the minimum, i.e., 326.4 K. In addition, as for multichip devices, if the temperature distribution of the chip is quite inhomogeneous, there will be thermal stress in chips, which is harmful. From Figure 10, the minimum temperature difference between the two heat sources is about 12.3 K when $a = b = 55$ mm. However, when $a = b = 35$ or 45 mm, the temperature difference is only 0.2 K larger than 12.3 K. On the other hand, the farther the discrete heat sources distribution is, the

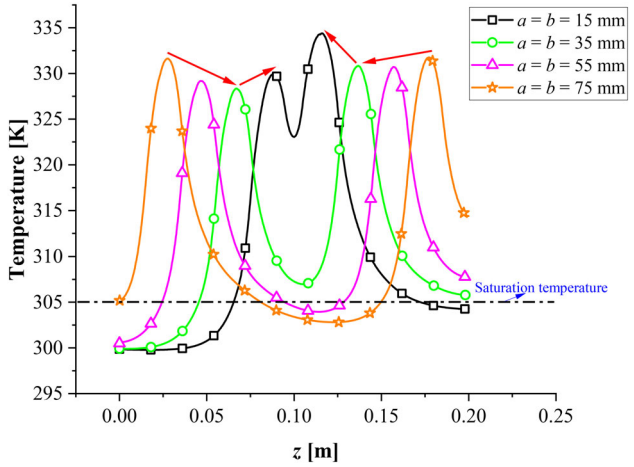

Figure 11. Temperature variation of channel inner wall when flow time is 6.5 s.

more space costs will be required. Therefore, considering the heat dissipation and space costs, $a = b = 35$ mm is the best relative distance between discrete heat sources in this study.

In order to explore the reason why the heat transfer performance is the best when $a = b = 35$ mm, the temperature variation along the inner channel wall is discussed. It can be seen from Figure 11 that there are two temperature peaks on each temperature variation curve, which correspond to the locations of two discrete heat sources. Heat can be transferred rapidly in the metal channel along the axial direction when heat sources are distributed discretely, so the temperature variations of two discrete heat sources increase first and then decrease. The average temperature of heat source 2 is higher than that of heat source 1 due to the thermal boundary layer development. Moreover, the inner wall temperature is minimum when $a = b = 35$ mm. According to Fourier heat conduction law, the temperature difference between the inner wall and outer wall is small in this study, so it also can be indicated from Figure 11 that heat transfer is the best when $a = b = 35$ mm. As shown in Figure 11, when the distance between two heat sources is too close (e.g., $a = b = 15$ mm), the superheat of the wall surface is high, and the heat will be concentrated, which is not conducive to heat transfer. However, the distance between two heat sources also shouldn't be too far, because the superheat of the wall is too low, the inner wall temperature is lower than the fluid saturation temperature (e.g., $a = b = 75$ mm), and the latent heat is not fully utilized. Only when $a = b = 35$ mm, the temperature distribution is appropriate, and the heat dissipation is the best compared with other conditions.

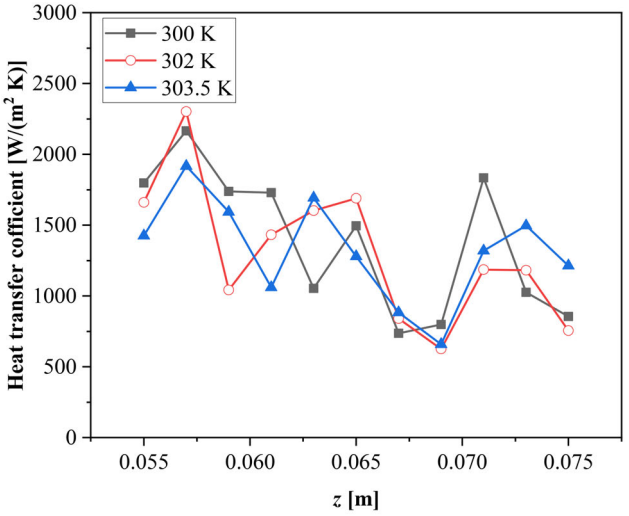

(a) around heat source 1

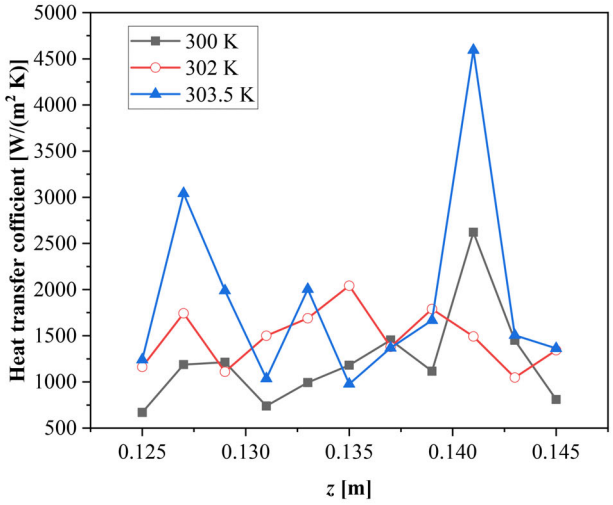

(b) around heat source 2

Figure 12. Heat transfer coefficients around heat source vary with inlet temperature when flow time is 6.5 s.

Effect of inlet temperature and channel diameter

The influence of inlet temperature on heat transfer for 3 mm channel, heat flux of 30000 W/m^2 and inlet velocity of 0.2 m/s is investigated in Figure 12. As seen from Figure 12(a), with the increase of inlet temperature, the heat transfer coefficient around heat source 1 does not increase significantly, but the heat transfer coefficient around heat source 2 shown in Figure 12(b) increases significantly. This is because when the inlet temperature increases, there is mainly saturated boiling instead of subcooled boiling in the channel and the single-phase flow will be reduced, in which the latent heat can be fully utilized. This phenomenon is especially obvious in the fluid near heat source 2 because of the preheating of heat source 1, which can be confirmed

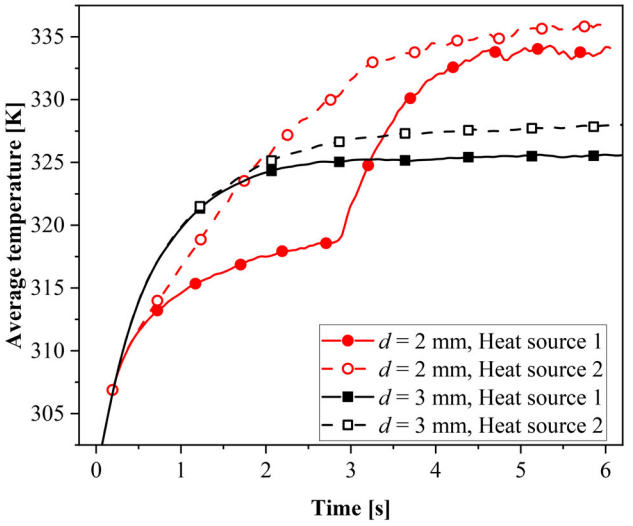

Figure 13. The average temperature of heat source varies with time in different channels.

by the corresponding flow pattern in Figure 6. As shown in Figure 6, there is mainly sub-cooled boiling and some immature bubbles in the fluid near heat source 1 even if inlet temperature increases, but bubbles flow and cap flow appear in the fluid near heat source 2 when inlet temperature increases.

In order to discuss the effect of channel diameter on heat transfer, the average temperature variations of heat source 1 and heat source 2 with time in different channels are shown in Figure 13. As shown in Figure 7, before flow boiling reaches the pseudo steady state, the flow pattern in the 2 mm channel is slug flow, so the average temperatures of heat source 1 and heat source 2 are both lower than that in the 3 mm channel before 1.5 s as illustrated in Figure 13. Due to the smaller channel diameter, the bubbles are easier to occupy the whole channel section and form intermittent flow in the channel as shown in Figure 8. In addition, as mentioned above, intermittent flow tends to form in the fluid near discrete heat sources especially heat source 2. Therefore, the average temperature of heat source 2 in the 2 mm channel is greater than that in the 3 mm channel first. Besides, the fluctuation of heat source average temperature in the small channel is more obvious than that in the 3 mm channel.

Pressure drop characteristics

For a good cooling system, not only excellent heat transfer efficiency but also low-pressure drop is expected. Pressure drop characteristics are necessary to be studied for selecting pumps and energy conservation. Therefore, the effects of the heat source distribution, inlet temperature and channel diameter

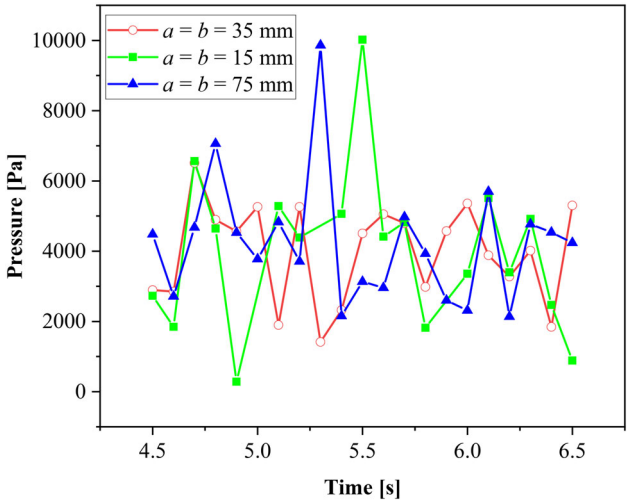

Figure 14. Pressure drop in the channel varies with time after flow boiling reaches the pseudo steady state when heat sources distribution is different.

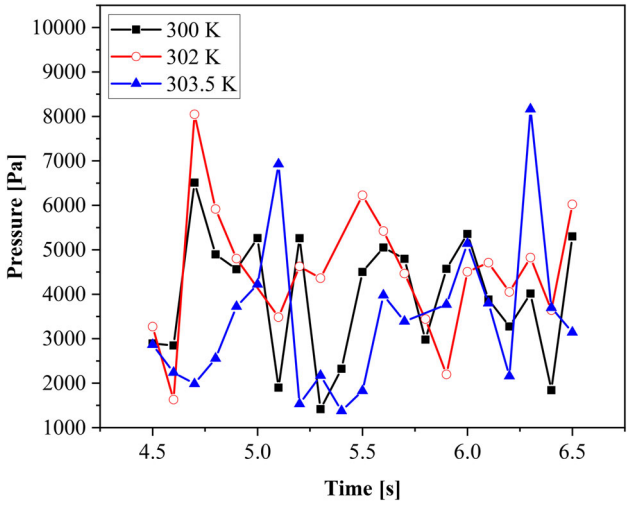

Figure 15. Pressure drop in the channel varies with time after flow boiling reaches the pseudo steady state when the inlet temperature of fluid is different.

on pressure drop are investigated when the flow boiling reaches the pseudo steady state.

Figures 14 and 15 demonstrate the pressure drop in the channel when heat source distribution and inlet fluid temperature are different. It can be seen that the pressure drop is fluctuating because there is two-phase flow in the channel. Moreover, the maximum pressure drop is below 10 kPa when channel diameter, heat flux, inlet velocity and inlet temperature are 3 mm, 30000 W/m^2, 0.2 m/s and 300 K − 303.5 K. Compared with other conditions, the pressure drop fluctuation in the channel is more stable when $a = b = 35$ mm as shown in Figure 14. Besides, the pressure drop in the 2 mm channel is discussed in Figure 16. Unlike the pressure drop in the 3 mm channel, pressure drop

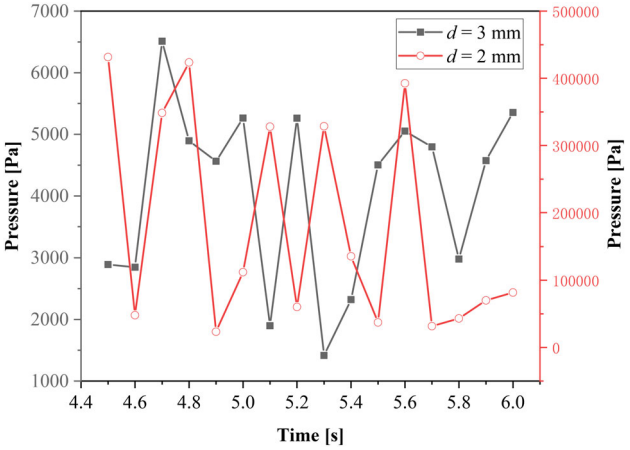

Figure 16. Pressure drop in the channel varies with time after flow boiling reaches the pseudo steady state when channel diameter is different.

fluctuation in the 2 mm channel is obvious and the maximum pressure drop is even up to 500 kPa, which is caused by slug flow and intermittent flow observed in the fluid near the discrete heat source in the 2 mm channel as shown in Figure 8.

Conclusions

A numerical method is performed to investigate the flow pattern, heat transfer performance and pressure drop characteristics of flow boiling with discrete heat sources in this study. Based on model validation, the influences of discrete heat source distribution, inlet temperature and channel diameter on flow pattern, heat transfer and pressure drop are discussed in detail. The main conclusions are drawn as follows:

1. The phenomenon of flow boiling in a mini-channel heated with discrete heat sources is different from that heated with a continuous heat source. The discrete heat source distribution is an important factor affecting the flow pattern. Intermittent flow tends to appear in the fluid near discrete heat sources especially heat source 2 which is far from the inlet.
2. With the increase of inlet fluid temperature and the decrease of channel diameter, there are more flow patterns, such as cap flow, slug flow, intermittent flow and annular flow. In addition, the flow pattern of R141b is sensitive to channel diameter.
3. It is necessary to optimize the discrete heat source distribution to improve heat transfer. The distance between discrete heat sources shouldn't be too close to avoid heat concentration, nor too far to make full use of latent heat. When $a = b = 35$ mm, the temperature distribution is

appropriate and heat dissipation is the best in the present study.

4. With the increase of inlet temperature, the heat transfer coefficients around heat source 1 do not increase significantly, while the preheating of heat source 1 makes the heat transfer coefficients around heat source 2 increase significantly with the increase of inlet temperature.
5. The pressure drop in the channel fluctuates due to the influence of bubbles. The maximum pressure drop is below 10 kPa when the channel diameter, heat flux, inlet velocity and inlet temperature are 3 mm, 30000 W/m^2, 0.2 m/s and 300 K-303.5 K. Moreover, the maximum pressure drop in the 2 mm channel is up to 500 kPa caused by slug flow and intermittent flow.

This work discussed the effects of discrete heat source distribution, inlet temperature and channel diameter on flow pattern, heat transfer and pressure drop. Conclusions obtained from this study are expected to design and optimize the cooling system of two-phase flow. The investigation on the effect of discrete heat sources can optimize the spatial distribution of discrete heat sources, and the studies of inlet temperature are useful for operating conditions design. Moreover, pressure drop characteristics obtained are helpful for selecting pumps and energy conservation.

Funding

This work was supported by the key project of National Natural Science Foundation of China (No. 52130609).

Notes on contributors

Ping Yang is a master student in the School of Energy and Power Engineering, Xi'an Jiaotong University, China, since 2020. She received her bachelor's degree from Xi'an Jiaotong University, China, in 2020. Her main research interests are the numerical and experimental study of flow boiling and thermal management of phase change materials.

Weihao Ling is a master student in the School of Energy and Power Engineering, Xi'an Jiaotong University, China, since 2021. He received his bachelor's degree from Xi'an Jiaotong University, China, in 2021. His main research interests are numerical and theoretical study of turbulence with the method of nonlinear dynamics.

Ke Tian is a Ph.D. student in the School of Energy and Power Engineering, Xi'an Jiaotong University, China, since 2019. He received his bachelor's degree and mater's degrees from Hebei University of Technology, China, in 2016 and 2019, respectively. His main research interests are numerical and experimental study of novel heat transfer enhancement technology.

Min Zeng is a Professor of School of Energy and Power Engineering, Xi'an Jiaotong University. He received his Ph.D. degree in Engineering Thermophysics from Xi'an Jiaotong University in 2004. He was awarded a scholarship from the Swedish Institute from September 1, 2011, to September 1, 2012 for postdoctoral research at Lund University. He was awarded New Century Excellent Talents in University of China. His main research interests are enhanced heat transfer, compact heat exchangers, solid oxide fuel cell, and numerical heat transfer and transport phenomena in porous media. He has published more than forty papers in international journals or conferences and was also authorized with 2 USA and 8 China Invention Patents.

Qiuwang Wang is a Professor in the School of Energy and Power Engineering, Xi'an Jiaotong University, China. He received his Ph.D. in Engineering Thermophysics from Xi'an Jiaotong University, China, in 1996. He then joined the faculty of the university and took the professor post in 2001. His main research interests include energy storage and saving, control and optimization of heat and mass transfer processes, heat transfer under extreme conditions, etc. He has also been author or coauthor of 4 books and more than 200 journal papers with H-index of 45. He has obtained more than 40 China Invention Patents and 5 US Patents.

References

[1] T. G. Karayiannis and M. M. Mahmoud, "Flow boiling in microchannels: fundamentals and applications," *Appl. Therm. Eng.*, vol. 115, pp. 1372–1397, Mar2017. DOI: 10.1016/j.applthermaleng.2016.08.063.

[2] B. Sumith, F. Kaminaga and K. Matsumura, "Saturated flow boiling of water in a vertical small diameter tube," *Exp. Therm. Fluid Sci.*, vol. 27, no. 7, pp. 789–801, Sept2003. DOI: 10.1016/S0894-1777(02)00317-5.

[3] G. Lillo, R. Mastrullo, A. W. Mauro and L. Viscito, "Flow boiling heat transfer, dry-out vapor quality and pressure drop of propane (R290): Experiments and assessment of predictive methods," *Int. J. Heat Mass*

Transf., vol. 126, no. part B, pp. 1236–1252, Nov2018. DOI: 10.1016/j.ijheatmasstransfer.2018.06.069.

[4] X. J. Niu, H. J. Yuan, C. Quan, B. F. Bai and L. Zhao, "Flow boiling heat transfer of R134a in a vertical helically coiled tube," *Heat Transf. Eng.*, vol. 40, no. 16, pp. 1393–1402, Oct2019. DOI: 10.1080/01457632.2018.1470304.

[5] U. Soupremanien, S. L. Person, M. Favre-Marinet and Y. Bultel, "Influence of the aspect ratio on boiling flows in rectangular mini-channels," *Exp. Therm. Fluid Sci.*, vol. 35, no. 5, pp. 797–809, Jul2011. DOI: 10.1016/j.expthermflusci.2010.06.014.

[6] M. R. Özdemir, M. M. Mahmoud and T. G. Karayiannis, "Flow boiling of water in a rectangular metallic microchannel," *Heat Transf. Eng.*, vol. 42, no. 6, pp. 492–516, 2021. DOI: 10.1080/01457632.2019.1707390.

[7] T. H. Yen, M. Shoji, F. Takemura, Y. Suzuki and N. Kasagi, "Visualization of convective boiling heat transfer in single microchannels with different shaped cross-sections," *Int. J. Heat Mass Transf.*, vol. 49, no. 21-22, pp. 3884–3894, Oct. 2006. DOI: 10.1016/j.ijheatmasstransfer.2005.12.024.

[8] D. Deng, W. Wan, Y. Tang, Z. Wan and D. Liang, "Experimental investigations on flow boiling performance of reentrant and rectangular microchannels-a comparative study," *Int. J. Heat Mass Transf.*, vol. 82, pp. 435–446, Mar2015. DOI: 10.1016/j.ijheatmasstransfer.2014.11.074.

[9] C. Kunkelmann and P. Stephan, "CFD simulation of boiling flows using the volume-of-fluid method within OpenFOAM," *Numer. Heat Tranf.. A-Appl.*, vol. 56, no. 8, pp. 631–646, 2009. DOI: 10.1080/10407780903423908.

[10] N. La Forgia, M. Fernandino and C. A. Dorao, "Numerical simulation of evaporation process of two-phase flow in small-diameter channels," *Heat Transf. Eng.*, vol. 35, no. 5, pp. 440–451, 2014. DOI: 10.1080/01457632.2013.832596.

[11] F. X. Huang, et al., "Numerical analysis on flow pattern and heat transfer characteristics of flow boiling in the mini-channels," *Numer Heat Tranf. B-Fundam.*, vol. 78, no. 4, pp. 221–247, Jul2020. DOI: 10.1080/10407790.2020.1787032.

[12] X. Yin, Y. S. Tian, D. Zhou and N. H. Wang, "Numerical study of flow boiling in an intermediate-scale vertical tube under low heat flux," *Appl. Therm. Eng.*, vol. 153, pp. 739–747, Mar2019. DOI: 10.1016/j.applthermaleng.2019.03.067.

[13] W. Lee, G. Son and H. Y. Yonn, "Direct numerical simulation of flow boiling in a finned microchannel," *Int. J. Heat Mass Transf.*, vol. 39, no. 9, pp. 1460–1466, Nov2012. DOI: 10.1016/j.icheatmasstransfer.2012.08.005.

[14] Y. Luo, et al., "Three-dimensional numerical simulation of saturated annular flow boiling in a narrow rectangular microchannel," *Int. J. Heat Mass Transf.*, vol. 149, pp. 119246, Mar2020. DOI: 10.1016/j.ijheatmasstransfer.2019.119246.

[15] Y. Shao, et al., "A numerical study on heat transfer of R410A during flow boiling," *Energy Procedia*, vol. 158, pp. 5414–5420, Feb. 2019. DOI: 10.1016/j.egypro.2019.01.608.

[16] T. J. Heindel, S. Ramadhyani and F. P. Incropera, "Liquid immersion cooling of a longitudinal array of discrete heat sources in protruding substrates. II. Forced convection boiling," *ASME J. Elec. Packaging*, vol. 114, no. 1, pp. 63–70, Mar. 1992. DOI: 10.1115/1.2905443.

[17] E. S. Cho, J. W. Choi, J. S. Yoon and M. S. Kim, "Modeling and simulation on the mass flow distribution in microchannel heat sinks with non-uniform heat flux conditions," *Int. J. Heat Mass Transf.*, vol. 53, no. 7-8, pp. 1341–1348, Mar. 2010. DOI: 10.1016/j.ijheatmasstransfer.2009.12.025.

[18] E. S. Cho, J. W. Choi, J. S. Yoon and M. S. Kim, "Experimental study on microchannel heat sinks considering mass flow distribution with non-uniform heat flux conditions," *Int. J. Heat Mass Transf.*, vol. 53, no. 9-10, pp. 2159–2168, Apr. 2010. DOI: 10.1016/j.ijheatmasstransfer.2009.12.026.

[19] S. N. Ritchey, J. A. Weibel and S. V. Garimella, "Local measurement of flow boiling heat transfer in an array of non-uniformly heated microchannels," *Int. J. Heat Mass Transf.*, vol. 71, pp. 206–216, Apr. 2014. DOI: 10.1016/j.ijheatmasstransfer.2013.12.012.

[20] K. Kurose, K. Miyata, Y. Hamamoto and H. Mori, "Flow boiling heat transfer and flow distribution of HFC32 and HFC134a in unequally heated parallel mini-channels," *Int. J. Refrig.*, vol. 119, pp. 305–315, Nov2020. DOI: 10.1016/j.ijrefrig.2020.05.011.

[21] K. Kurose, W. Noboritate, S. Sakai, K. Miyata and Y. Hamamoto, "An experimental study on flow boiling heat transfer of R410A in parallel two mini-channels heated unequally by high-temperature fluid," *Appl. Therm. Eng.*, vol. 178, pp. 115669, Sep. 2020. DOI: 10.1016/j.applthermaleng.2020.115669.

[22] C. Hu, et al., "Numerical investigation on two-phase flow heat transfer performance and instability with discrete heat sources in parallel channels," *Energies*, vol. 14, no. 15, pp. 4408, Aug. 2021. DOI: 10.3390/en14154408.

[23] J. U. Brackbill, D. B. Kothe and C. Zemach, "A continuum method for modeling surface tension," *J. Comput. Phys.*, vol. 100, no. 2, pp. 335–354, Jun. 1992. DOI: 10.1016/0021-9991(92)90240-Y.

[24] W. H. Lee, "A pressure iteration scheme for two-phase flow modeling," in *Multiphase Transport. Fundamentals, Reactor Safety, Applications*, ed., T.N. Veziroglu. Washington, DC: Hemisphere Publishing, 1980, pp. 407–432.

[25] Z. Yang, X. F. Peng and P. Ye, "Numerical and experimental investigation of two-phase flow during boiling in a coiled tube," *Int. J. Heat Mass Transf.*, vol. 51, no. 5-6, pp. 1003–1016, Mar2008. DOI: 10.1016/j.ijheatmasstransfer.2007.05.025.

[26] D. Youngs, "Time-dependent multi-material flow with large fluid distortion," in *Numerical Methods for Fluid Dynamics*, ed., K.W. Morton and M.J. Baines, New York: Academic Press, 1982, pp. 273–285.

[27] S. Lin, P. A. Kew and K. Cornwell, "Two-phase heat transfer to a refrigerant in a 1 mm diameter tube," *Int. J. Refrig.*, vol. 24, no. 1, pp. 51–56, Jan. 2001. DOI: 10.1016/S0140-7007(00)00057-8.